High-energy hadronic total cross sections, Wilson loop correlators and the QCD spectrum

Enrico Meggiolaro

Dipartimento di Fisica "Enrico Fermi", Università di Pisa,
and I.N.F.N., Sezione di Pisa

2nd Italian Workshop on Hadron Physics and Non-Perturbative QCD
(NPQCD 2017)
Pollenzo (CN), May 22nd–24th, 2017

Based on:
M. Giordano and EM, *JHEP* **03** (2014) 002 [arXiv:1311:3133 [hep-ph]]
M. Giordano and EM, *PLB* **744** (2015) 263 [arXiv:1411.0553 [hep-ph]]
M. Giordano, EM, and P.V.R.G. Silva, arXiv:1703.00244 [hep-ph]

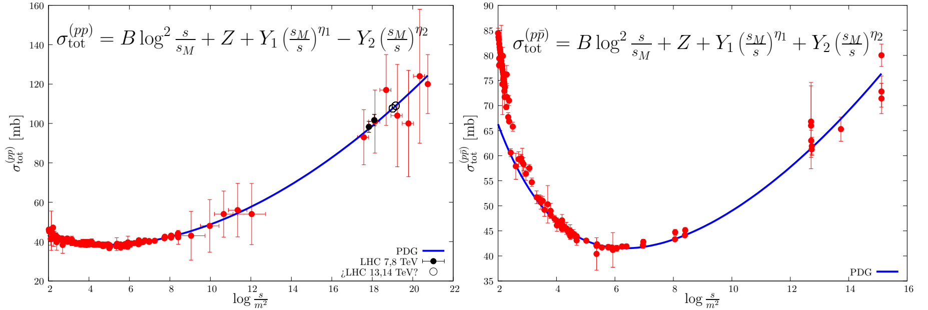

[TOTEM (2013)][PDG (2014)]

$$\sigma_{tot}^{(hh)}(s) \sim B\log^2 s$$

Universal $B \simeq 0.3\,\mathrm{mb}$, independent of the colliding hadrons [Ishida, Igi (2002)]

Consistent with Froissart bound (unitarity + mass gap) [Froissart (1961)]

$$\sigma_{tot}^{(hh)}(s) \leq \frac{\pi}{m_\pi^2}\log^2\frac{s}{s_0}$$

Soft High-Energy Scattering and Total Cross Sections

Total cross sections related to forward elastic amplitudes via optical theorem

$$\sigma_{\rm tot} \underset{s\to\infty}{\simeq} \frac{1}{s}\,{\rm Im}\,\mathcal{M}(s,t=0)$$

Soft high-energy hadron-hadron scattering: $s\to\infty\,,\ |t|\le 1\,{\rm GeV}^2$
One of the oldest unsolved problems of strong interactions

Impact parameter representation $[t=-\vec{q}_\perp^{\,2}]$

$$\mathcal{M}(s,t) = i\;2s\int d^2\vec{b}_\perp e^{i\vec{q}_\perp\cdot\vec{b}_\perp} A(s,\vec{b}_\perp)$$

$$\sigma_{\rm tot} = 2\,{\rm Re}\int d^2\vec{b}_\perp\, A(s,\vec{b}_\perp)$$

Unitarity: $|A(s,\vec{b}_\perp)-1|\le 1$

Soft High-Energy Scattering and Total Cross Sections

Total cross sections related to forward elastic amplitudes via optical theorem

$$\sigma_{\rm tot} \underset{s\to\infty}{\simeq} \frac{1}{s}\,{\rm Im}\,\mathcal{M}(s,t=0)$$

Soft high-energy hadron-hadron scattering: $s \to \infty\,,\ |t| \le 1\,{\rm GeV}^2$
One of the oldest unsolved problems of strong interactions

Impact parameter representation for unpolarised scattering $[t = -\vec{q}_\perp^{\,2}]$

$$\mathcal{M}(s,t) = i\ 2s \int d^2\vec{b}_\perp e^{i\vec{q}_\perp\cdot\vec{b}_\perp} A(s,\vec{b}_\perp) \ = \ i\ 4\pi s \int_0^\infty db b\, J_0(bq) A(s,b)$$

$$\sigma_{\rm tot} = 2\,{\rm Re}\,\int d^2\vec{b}_\perp\, A(s,\vec{b}_\perp) \ = \ 4\pi\,{\rm Re}\,\int_0^\infty db b\, A(s,b)$$

Unitarity: $|A(s,\vec{b}_\perp) - 1| \le 1$ $\qquad |A(s,b) - 1| \le 1$

How to Obtain a Rising Total Cross Section

Typical shape: $A \to 0$ at large b, for $b > b_c(s)$ the amplitude is "negligible"

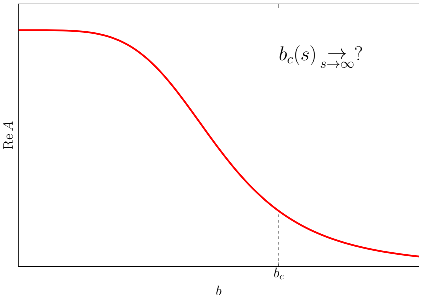

$\sigma_{\rm tot} \sim b_c(s)^2$: how does b_c change with s?

How to Obtain a Rising Total Cross Section

Typical shape: $A \to 0$ at large b, for $b > b_c(s)$ the amplitude is "negligible"

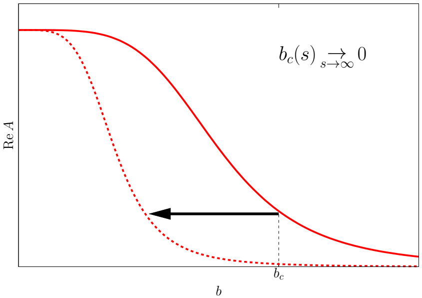

$\sigma_{\rm tot} \sim b_c(s)^2$: how does b_c change with s? $b_c(s) \to 0$

$$\sigma_{\rm tot} \to 0$$

How to Obtain a Rising Total Cross Section

Typical shape: $A \to 0$ at large b, for $b > b_c(s)$ the amplitude is "negligible"

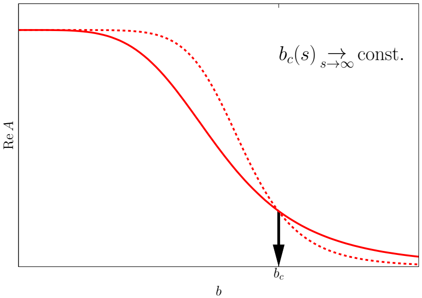

$\sigma_{\text{tot}} \sim b_c(s)^2$: how does b_c change with s? $b_c(s) \to \text{const.}$

$$\sigma_{\text{tot}} \to \text{const.}$$

How to Obtain a Rising Total Cross Section

Typical shape: $A \to 0$ at large b, for $b > b_c(s)$ the amplitude is "negligible"

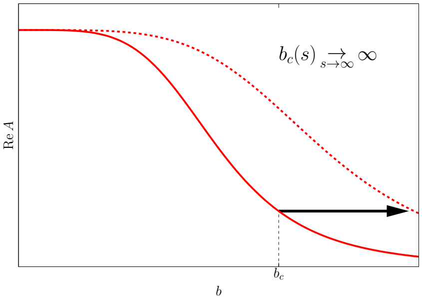

$\sigma_{\rm tot} \sim b_c(s)^2$: how does b_c change with s? $b_c(s) \to \infty$

$$\sigma_{\rm tot} = 4\pi b_c(s)^2 \,{\rm Re} \int_0^\infty dx\, x\, A(s, b_c(s)x) \to 4\pi b_c(s)^2 C$$

How to Obtain a Rising Total Cross Section

Typical shape: $A \to 0$ at large b, for $b > b_c(s)$ the amplitude is "negligible"

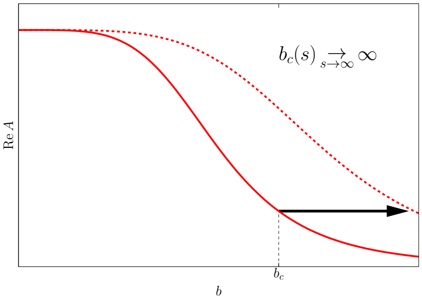

$\sigma_{\rm tot} \sim b_c(s)^2$: how does b_c change with s? $b_c(s) \to \infty$

$$\sigma_{\rm tot} = 4\pi b_c(s)^2 \,\mathrm{Re} \int_0^\infty dx\, x\, A(s, b_c(s)x) \to 4\pi b_c(s)^2 C$$

- $b_c(s)$ gives the energy dependence
- large b ($\gg m^{-1}$) is relevant

Soft High-Energy Scattering and QCD

QCD: fundamental theory, should explain the rise of total cross sections

$|t| \lesssim 1\mathrm{GeV}^2$, PT not fully reliable $\rightarrow$ NP approach [Nachtmann (1991)]

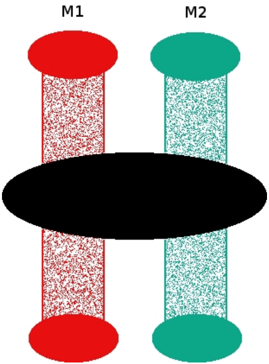

1. Partonic description of hadrons over a small time–window ($\sim 2\mathrm{fm}$)
2. Partons do not split or annihilate, treated as in/out states of a scattering process
3. Lightlike trajectories approx. unchanged in the process, only soft gluon exchange
4. Hadronic amplitude after folding with hadronic wave function

Soft High-Energy Scattering and QCD

QCD: fundamental theory, should explain the rise of total cross sections

$|t| \lesssim 1\mathrm{GeV}^2$, PT not fully reliable $\to$ NP approach [Nachtmann (1991)]

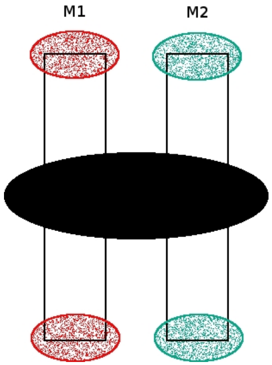

1. Partonic description of hadrons over a small time–window ($\sim 2\mathrm{fm}$)
2. Partons do not split or annihilate, treated as in/out states of a scattering process
3. Lightlike trajectories approx. unchanged in the process, only soft gluon exchange
4. Hadronic amplitude after folding with hadronic wave function

Soft High-Energy Scattering and QCD

QCD: fundamental theory, should explain the rise of total cross sections

$|t| \lesssim 1\mathrm{GeV}^2$, PT not fully reliable $\to$ NP approach [Nachtmann (1991)]

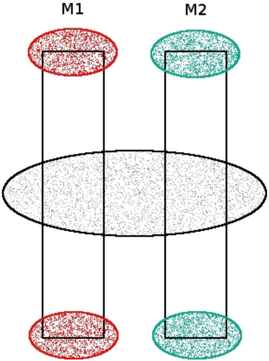

1. Partonic description of hadrons over a small time–window ($\sim 2\mathrm{fm}$)
2. Partons do not split or annihilate, treated as in/out states of a scattering process
3. Lightlike trajectories approx. unchanged in the process, only soft gluon exchange
4. Hadronic amplitude after folding with hadronic wave function

Nonperturbative Approach

Partonic scattering amplitudes from the correlation function of infinite lightlike Wilson lines [Nachtmann (1991)]

To avoid IR divergences → hadronic amplitudes

- mesons as wave packets of transverse colourless dipoles
- dipole scattering amplitudes from the correlation function of infinite lightlike Wilson loops [Dosch *et al.* (1996)]

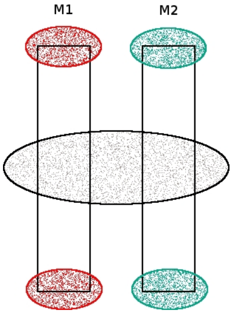

Intermediate regularisation: finite hyperbolic angle χ and length $2T$ [Verlinde, Verlinde (1993)]

Extends to baryon-baryon scattering adopting a quark-diquark description[Rueter, Dosch (1996)]

Meson-Meson (Dipole-Dipole) Elastic Scattering

Elastic meson-meson from dipole-dipole scattering [Dosch *et al.* (1996)]

$$A(s, \vec{b}_\perp) = \langle\langle A^{(dd)}(s, \vec{b}_\perp; \nu_1, \nu_2) \rangle\rangle$$

$\nu_i = (f_i, \vec{R}_{i\perp})$, f_i longitudinal momentum fraction, $\vec{R}_{i\perp}$ transverse size

$\langle\langle \ldots \rangle\rangle$: average over dipole variables $\nu_{1,2}$ with mesonic wave functions, i.e.,

$$\langle\langle F \rangle\rangle = \int_0^1 df_1 \int d^2\vec{R}_{1\perp} \, |\psi_1(\nu_1)|^2 \int_0^1 df_2 \int d^2\vec{R}_{2\perp} \, |\psi_2(\nu_2)|^2 \, F(\nu_1, \nu_2) \qquad (\langle\langle 1 \rangle\rangle = 1)$$

dd scattering amplitude in *b*-space $\leftrightarrow$ Wilson-loop correlation function

$$-A^{(dd)}(s, \vec{b}_\perp; \nu_1, \nu_2) \underset{s\to\infty}{\simeq} \mathcal{C}_M(\chi; \vec{b}_\perp; \nu_1, \nu_2) \qquad \chi \underset{s\to\infty}{\simeq} \log \frac{s}{m^2}$$

$$\mathcal{G}_M(\chi; T; \vec{b}_\perp; \nu_1, \nu_2) \equiv \frac{\langle \mathcal{W}_{\mathcal{C}_1} \mathcal{W}_{\mathcal{C}_2} \rangle}{\langle \mathcal{W}_{\mathcal{C}_1} \rangle \langle \mathcal{W}_{\mathcal{C}_2} \rangle} - 1 \qquad \mathcal{C}_M \equiv \lim_{T\to\infty} \mathcal{G}_M$$

$\langle \ldots \rangle$: expectation value in the (Minkowskian) QCD functional integral formalism

Wilson Loop Correlation Function

$$\mathcal{W}_{\mathcal{C}}[A] \equiv \frac{1}{N_c} \mathrm{Tr}\mathcal{P} \exp\{-ig \oint_{\mathcal{C}} A_\mu(X) dX^\mu\}$$

$$\mathcal{G}_M(\chi; T; \vec{b}_\perp; \nu_1, \nu_2) \equiv \frac{\langle \mathcal{W}_{\mathcal{C}_1} \mathcal{W}_{\mathcal{C}_2} \rangle}{\langle \mathcal{W}_{\mathcal{C}_1} \rangle \langle \mathcal{W}_{\mathcal{C}_2} \rangle} - 1 \,, \qquad \mathcal{C}_M \equiv \lim_{T \to \infty} \mathcal{G}_M$$

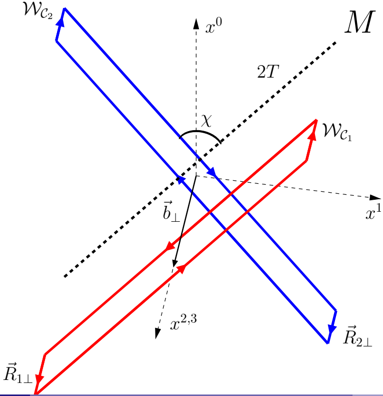

Wilson Loop Correlation Function

NP techniques available in Euclidean space ($\langle \ldots \rangle_E$)

$\Rightarrow$ Euclidean formulation [EM (1997), EM (2005)]

$$\mathcal{G}_E(\theta; T; \vec{b}_\perp; \nu_1, \nu_2) \equiv \frac{\langle \mathcal{W}_{\mathcal{C}_1} \mathcal{W}_{\mathcal{C}_2} \rangle_E}{\langle \mathcal{W}_{\mathcal{C}_1} \rangle_E \langle \mathcal{W}_{\mathcal{C}_2} \rangle_E} - 1\,, \qquad \mathcal{C}_E \equiv \lim_{T\to\infty} \mathcal{G}_E$$

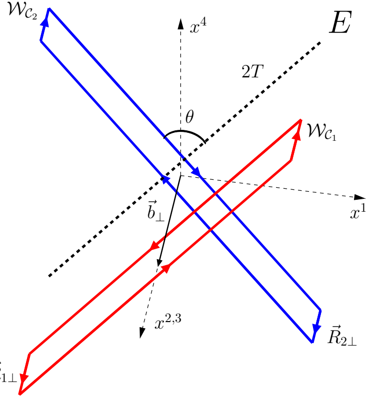

Analytic Continuation to Euclidean Space

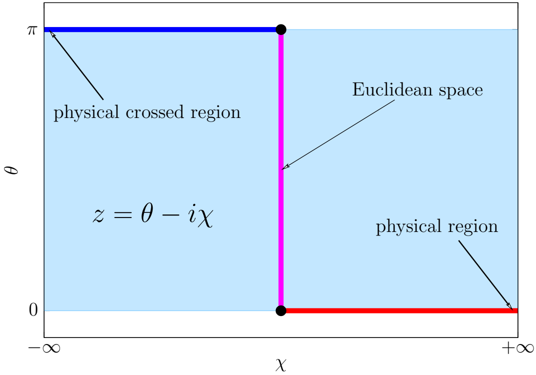

Analytic continuation relations [EM (2005), Giordano, EM (2009)]

$$\mathcal{C}_M(\chi) = \mathcal{C}_E(\theta \to -i\chi)$$

AC + Euclidean symmetries ⇒ crossing relations [Giordano, EM (2006)]

$$\mathcal{C}_M(i\pi - \chi; \vec{R}_{1\perp}, \vec{R}_{2\perp}) = \mathcal{C}_M(\chi; \vec{R}_{1\perp}, -\vec{R}_{2\perp})$$

Nonperturbative Models

Euclidean formulation opens the way to NP techniques:

- Stochastic Vacuum Model [Berger, Nachtmann (1999), Shoshi *et al.* (2003)]
- Instanton Liquid Model [Shuryak, Zahed (2000), Giordano, EM (2010)]
- AdS/CFT Correspondence [Janik, Peschanski (2000a,b), Giordano, Peschanski (2010)]
- Lattice Gauge Theory [Giordano, EM (2008), Giordano, EM (2010)]

Stochastic Vacuum Model (SVM)	$\mathcal{C}_E = \frac{2}{3}e^{-\frac{1}{3}\cot\theta\, K_{\mathrm{SVM}}} + \frac{1}{3}e^{\frac{2}{3}\cot\theta\, K_{\mathrm{SVM}}} - 1$
Instanton Liquid Model (ILM)	$\mathcal{C}_E = \frac{K_{\mathrm{ILM}}}{\sin\theta}$
Perturbation Theory (PT)	$\mathcal{C}_E = K_{\mathrm{PT}}\cot^2\theta$
ILM + PT (ILMp)	$\mathcal{C}_E = \frac{K_{\mathrm{ILMp}}}{\sin\theta} + K'_{\mathrm{ILMp}}(\cot\theta)^2$
AdS/CFT correspondence	$\mathcal{C}_E = e^{\frac{K_{\mathrm{AdS}}}{\sin\theta} + K'_{\mathrm{AdS}}\cot\theta + K''_{\mathrm{AdS}}\cos\theta\cot\theta} - 1$

NP Models, Lattice Results and Rising Cross Sections

Lattice calculations give "true" prediction of QCD (within errors) $\Rightarrow$ test analytic NP calculations

Are the analytic NP calculations compatible with the lattice results?

- SVM/ILM do not match/fit well the data and $\sigma_{tot}^{\mathrm{SVM,ILM}} \underset{s\to\infty}{\to} \mathrm{const.}$
- ILM+PT gives improved best fits but $\sigma_{tot}^{\mathrm{ILMp}} \underset{s\to\infty}{\to} \mathrm{const.}$
- AdS/CFT: $\sigma_{tot} \propto s^{\frac{1}{3}}$ but for onium-onium scattering in $\mathcal{N} = 4$ SYM [Giordano, Peschanski (2010)]

Are the lattice results compatible with rising total cross sections?

- More general fits, but care is needed because of the AC
- Constrain admissible fitting functions with physical requirements (unitarity, crossing symmetry,. . .)
- Parameterisations fitting well the data and leading to rising total cross sections exist [Giordano, EM, Moretti (2012)]

NP Models, Lattice Results and Rising Cross Sections

Lattice calculations give "true" prediction of QCD (within errors) $\Rightarrow$ test analytic NP calculations

Are the analytic NP calculations compatible with the lattice results?

- SVM/ILM do not match/fit well the data and $\sigma_{tot}^{\mathrm{SVM,ILM}} \underset{s\to\infty}{\to} \mathrm{const.}$
- ILM+PT gives improved best fits but $\sigma_{tot}^{\mathrm{ILMp}} \underset{s\to\infty}{\to} \mathrm{const.}$
- AdS/CFT: $\sigma_{tot} \propto s^{\frac{1}{3}}$ but for onium-onium scattering in $\mathcal{N} = 4$ SYM [Giordano, Peschanski (2010)]

Are the lattice results compatible with rising total cross sections?

- More general fits, but care is needed because of the AC
- Constrain admissible fitting functions with physical requirements (unitarity, crossing symmetry,...)
- Parameterisations fitting well the data and leading to rising total cross sections exist [Giordano, EM, Moretti (2012)]

NP Models and Lattice Results

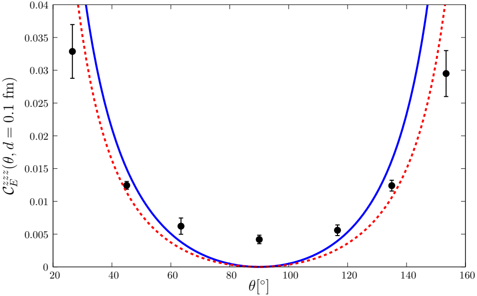

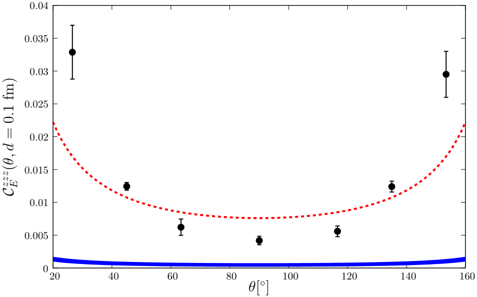

Lattice calculations give "true" prediction of QCD (within errors) $\Rightarrow$ test analytic NP calculations

Numerical predictions and fits of model functions of SVM (top) and ILM (bottom) to lattice data

Lattice setup:

- Wilson action for $SU(3)$ gauge theory (*quenched* QCD)
- 16^4 hypercubic lattice, $a \simeq 0.1\,\mathrm{fm}$
- longest available loops ($L \simeq 8$)
- $\cot\theta = 0, \pm 1/2, \pm 1, \pm 2$
- $|\vec{r}_{1,2\perp}| = 1a$, $|\vec{d}_\perp| = 0, 1, 2a$
- "zzz": $\vec{d}_\perp \parallel \vec{r}_{1\perp} \parallel \vec{r}_{2\perp}$
- "zyy": $\vec{d}_\perp \perp \vec{r}_{1\perp} \parallel \vec{r}_{2\perp}$
- "ave": average over orientations

Rising Cross Sections From the Lattice

Parameterisation: $\mathcal{C}_E = e^{K_E} - 1$

$$K_E = \sum_i f_i(\theta) g_i(\vec{b}_\perp; \nu_1, \nu_2)$$

Unitarity constraint: $\mathrm{Re}\, K_M \le 0$

$$[K_M(\chi) = K_E(\theta \to -i\chi)]$$

At large b, $K_E, K_M \sim (\sum) e^{-\mu b}$

If $K_M \sim \chi^p e^{n\chi}\, e^{-\mu b} \sim (\log s)^p s^n\, e^{-\mu b}$

$$\sigma_{\rm tot}^{(hh)} \sim B \log^2 s$$

with $\quad B = \frac{2\pi n^2}{\mu^2} \quad$ **universal**

Estimate of B fairly agrees with $B_{\rm exp}$

(although *quenched* and with rather large errors)

Where does this come from?

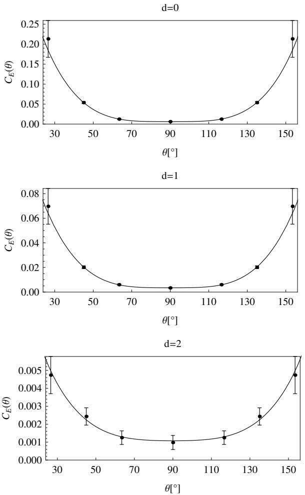

$$K_E = \frac{K_1}{\sin\theta} + K_2\left(\tfrac{\pi}{2} - \theta\right)^3 \cos\theta$$

Summary and Questions

- $\sigma_{\rm tot} \sim$ large-b behaviour of elastic scattering amplitudes in impact-parameter space $A(s, b)$
- QCD at large-s and small-t: $A(s, b) \sim$ Wilson loop correlation function
- Analytic models fail to reproduce the lattice data and to capture the rising behaviour of $\sigma_{\rm tot}$
- Lattice data compatible with rising behaviour, but large arbitrariness in the parameterisations

1. What are the large-s and large-b behaviour of $A(s, b)$?
2. What sets the physical scale in $\sigma_{\rm tot}$?
3. How does $\sigma_{\rm tot}$ relate to the hadronic spectrum?

Relating Total Cross Sections and the QCD Spectrum

How to extract θ and b dependencies?

Basic idea: insert a complete set of states between the Wilson loops

$$\langle 0|\hat{\mathcal{O}}_1(t)\hat{\mathcal{O}}_2(0)|0\rangle = \sum_n e^{-E_n t}\langle 0|\hat{\mathcal{O}}_1(0)|n\rangle\langle n|\hat{\mathcal{O}}_2(0)|0\rangle$$

Complications: nonlocal operators, nontrivial angular dependence

Use asymptotic states with simple transformation properties

$$|\alpha\rangle = |\{n_a(\alpha)\}, \{\vec{p}\}, \{s_3\}\rangle$$

$\{n_a(\alpha)\}$: particle content, $\{\vec{p}\}$: momenta, $\{s_3\}$: 3rd component of spin

$$\sum_n |n\rangle\langle n| = \sum_\alpha \mathcal{P}_\alpha \sum_{\{s_3\}_\alpha} \int d\Omega_\alpha \, |\alpha\rangle\langle\alpha|$$

$\mathcal{P}_\alpha = \frac{1}{\prod_a n_a(\alpha)!}$ symmetry factor, $d\Omega_\alpha$ phase space measure

Sketch of Derivation

Rotate Euclidean time along the impact parameter (equivalent description)

$$\mathcal{G}_E(\theta; T; \vec{b}_\perp; \nu_1, \nu_2) \equiv \frac{\langle \mathcal{W}_{\mathcal{C}_1} \mathcal{W}_{\mathcal{C}_2} \rangle_E}{\langle \mathcal{W}_{\mathcal{C}_1} \rangle_E \langle \mathcal{W}_{\mathcal{C}_2} \rangle_E} - 1$$

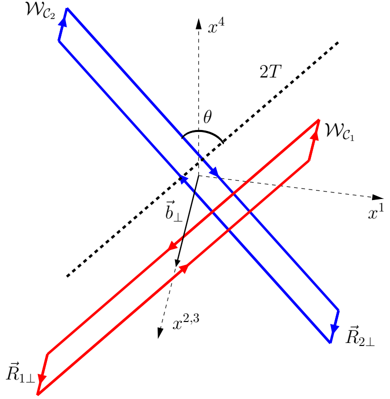

Rotate Euclidean time along the impact parameter (equivalent description)

$$\tilde{\mathcal{G}}_E(\theta; T; b; \nu_1, \nu_2) \equiv \frac{\langle \mathcal{W}_{\tilde{\mathcal{C}}_1} \mathcal{W}_{\tilde{\mathcal{C}}_2} \rangle_E}{\langle \mathcal{W}_{\tilde{\mathcal{C}}_1} \rangle_E \langle \mathcal{W}_{\tilde{\mathcal{C}}_2} \rangle_E} - 1$$

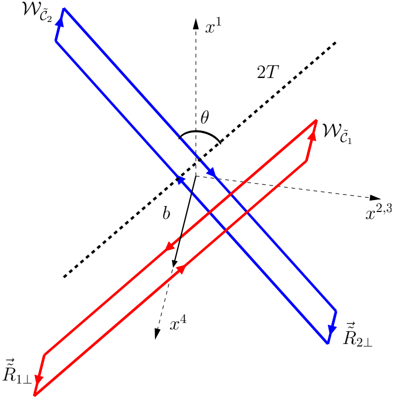

Sketch of Derivation

Use Wilson loop *operators*

$$\tilde{\mathcal{G}}_E(\theta; T; b; \nu_1, \nu_2) \equiv \frac{\langle \mathcal{W}_{\tilde{\mathcal{C}}_1} \mathcal{W}_{\tilde{\mathcal{C}}_2} \rangle_E}{\langle \mathcal{W}_{\tilde{\mathcal{C}}_1} \rangle_E \langle \mathcal{W}_{\tilde{\mathcal{C}}_2} \rangle_E} - 1 = \frac{\langle 0 | T\{\hat{\mathcal{W}}_{\tilde{\mathcal{C}}_1} \hat{\mathcal{W}}_{\tilde{\mathcal{C}}_2}\} | 0 \rangle}{\langle 0 | \hat{\mathcal{W}}_{\tilde{\mathcal{C}}_1} | 0 \rangle \langle 0 | \hat{\mathcal{W}}_{\tilde{\mathcal{C}}_2} | 0 \rangle} - 1$$

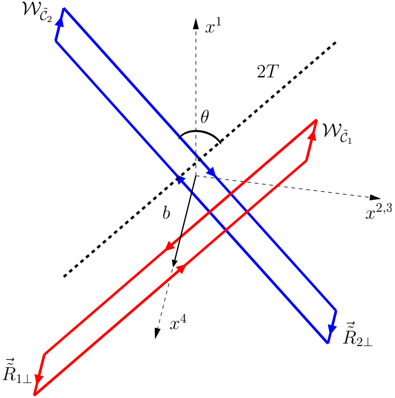

Sketch of Derivation

Consider loops with no temporal overlap ($b > b_0$)

$$\tilde{\mathcal{G}}_E(\theta; T; b; \nu_1, \nu_2) \equiv \frac{\langle \mathcal{W}_{\tilde{\mathcal{C}}_1} \mathcal{W}_{\tilde{\mathcal{C}}_2} \rangle_E}{\langle \mathcal{W}_{\tilde{\mathcal{C}}_1} \rangle_E \langle \mathcal{W}_{\tilde{\mathcal{C}}_2} \rangle_E} - 1 = \frac{\langle 0 | \hat{\mathcal{W}}_{\tilde{\mathcal{C}}_1} \hat{\mathcal{W}}_{\tilde{\mathcal{C}}_2} | 0 \rangle}{\langle 0 | \hat{\mathcal{W}}_{\tilde{\mathcal{C}}_1} | 0 \rangle \langle 0 | \hat{\mathcal{W}}_{\tilde{\mathcal{C}}_2} | 0 \rangle} - 1$$

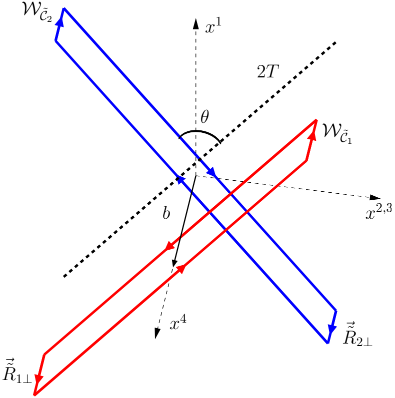

Sketch of Derivation

Insert a complete set of states

$$\tilde{\mathcal{G}}_E(\theta; T; b; \nu_1, \nu_2) = \frac{\langle 0|\hat{\mathcal{W}}_{\tilde{\mathcal{C}}_1}\hat{\mathcal{W}}_{\tilde{\mathcal{C}}_2}|0\rangle}{\langle 0|\hat{\mathcal{W}}_{\tilde{\mathcal{C}}_1}|0\rangle\langle 0|\hat{\mathcal{W}}_{\tilde{\mathcal{C}}_2}|0\rangle} - 1 = \sum_{n\neq 0} \frac{\langle 0|\hat{\mathcal{W}}_{\tilde{\mathcal{C}}_1}|n\rangle}{\langle 0|\hat{\mathcal{W}}_{\tilde{\mathcal{C}}_1}|0\rangle}\frac{\langle n|\hat{\mathcal{W}}_{\tilde{\mathcal{C}}_2}|0\rangle}{\langle 0|\hat{\mathcal{W}}_{\tilde{\mathcal{C}}_2}|0\rangle}$$

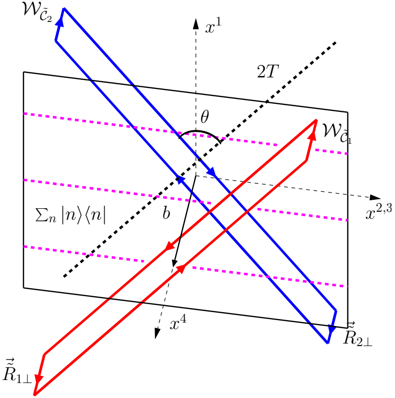

Sketch of Derivation

Rotate around 3-axis and translate centres to the origin, $|n_{\pm\frac{\theta}{2}}\rangle = e^{\pm i\hat{J}_3\frac{\theta}{2}}|n\rangle$

$$\tilde{\mathcal{G}}_E(\theta; T; b; \nu_1, \nu_2) = \sum_{n\neq 0} e^{-bE_n} e^{i\theta S_{3n}} \frac{\langle 0|\hat{\mathcal{W}}_0(\nu_1)|n_{\frac{\theta}{2}}\rangle}{\langle 0|\hat{\mathcal{W}}_0(\nu_1)|0\rangle} \frac{\langle n_{-\frac{\theta}{2}}|\hat{\mathcal{W}}_0(\nu_2)|0\rangle}{\langle 0|\hat{\mathcal{W}}_0(\nu_2)|0\rangle}$$

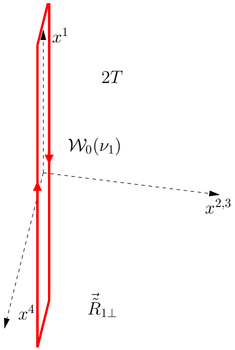

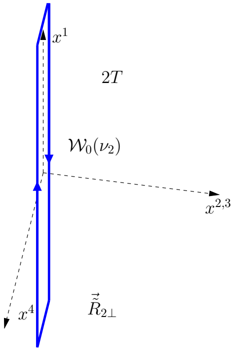

Sketch of Derivation

Rotate around 3-axis and translate centres to the origin, $|n_{\pm\frac{\theta}{2}}\rangle = e^{\pm i\hat{J}_3\frac{\theta}{2}}|n\rangle$

$$\tilde{\mathcal{G}}_E(\theta; T; b; \nu_1, \nu_2) = \sum_{n\neq 0} e^{-bE_n} e^{i\theta S_{3n}} \frac{\langle 0|\hat{\mathcal{W}}_0(\nu_1)|n_{\frac{\theta}{2}}\rangle}{\langle 0|\hat{\mathcal{W}}_0(\nu_1)|0\rangle} \frac{\langle n_{-\frac{\theta}{2}}|\hat{\mathcal{W}}_0(\nu_2)|0\rangle}{\langle 0|\hat{\mathcal{W}}_0(\nu_2)|0\rangle}$$

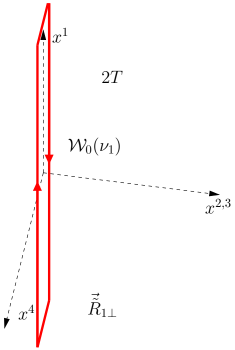

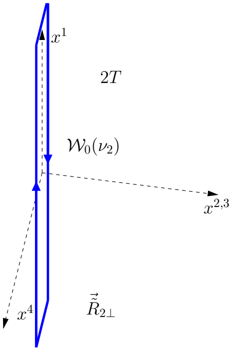

Sketch of Derivation

Take $T \to \infty$

$$\tilde{\mathcal{C}}_E(\theta; b; \nu_1, \nu_2) = \sum_{n \neq 0} e^{-bE_n} e^{i\theta S_{3n}} \frac{\langle 0|\hat{\mathcal{W}}_0(\nu_1)|n_{\frac{\theta}{2}}\rangle}{\langle 0|\hat{\mathcal{W}}_0(\nu_1)|0\rangle} \frac{\langle n_{-\frac{\theta}{2}}|\hat{\mathcal{W}}_0(\nu_2)|0\rangle}{\langle 0|\hat{\mathcal{W}}_0(\nu_2)|0\rangle}$$

$$= \sum_{\alpha \neq 0} \mathcal{P}_\alpha \sum_{\{s_3\}_\alpha} e^{i\theta S_{3\alpha}} \int d\Omega_\alpha \, e^{-bE_\alpha} W_\alpha^+(\{\vec{p}_{\frac{\theta}{2}}\}, \{s_3\}; \nu_1) W_\alpha^-(\{\vec{p}_{-\frac{\theta}{2}}\}, \{s_3\}; \nu_2)$$

E_α, $S_{3\alpha}$: total energy and 3rd component of spin in state α

$\{\vec{p}_{\pm\frac{\theta}{2}}\}$: all momenta rotated around 3-axis

Selection rule: $W_\alpha^\pm$ nonzero only for vanishing discrete charges (electric charge, baryon number, strangeness,...)

$$Q = B = S = \ldots = 0$$

Asymptotic Behaviour of the Correlator

At large χ and large b, using $\mathcal{C}_M(\chi;\vec{b}_\perp;\nu_1,\nu_2) = \tilde{\mathcal{C}}_E(-i\chi;b;\nu_1,\nu_2)$

$$\mathcal{C}_M(\chi;\vec{b}_\perp;\nu_1,\nu_2) \underset{\chi\to\infty,\, b\to\infty}{\sim} \sum_{\alpha\neq 0} \mathcal{P}_\alpha i^{N_\alpha} \mathcal{F}_\alpha^+(\nu_1)\mathcal{F}_\alpha^-(\nu_2) \prod_a {w_a}^{n_a(\alpha)}$$

up to $\mathcal{O}(e^{-\chi})$ and $\mathcal{O}(b^{-1})$

$$w_a(\chi,b) = \frac{1}{\sqrt{2\pi b m^{(a)}}} e^{\chi[s^{(a)}-1]} e^{-bm^{(a)}} = \frac{1}{\sqrt{2\pi b m^{(a)}}} e^{[R_{\rm eff}^{(a)}(s)-b]m^{(a)}}$$

Reminiscent of exchange of spin-J particle $\to$ contribution $\propto s^{J-1}$

Contribution of state α non-negligible only for

$$b \lesssim R_{\rm eff}^{[\alpha]} = \frac{\sum_a n_a(\alpha) m^{(a)} R_{\rm eff}^{(a)}(s)}{\sum_a n_a(\alpha) m^{(a)}} \qquad R_{\rm eff}^{(a)}(s) \equiv \frac{s^{(a)}-1}{m^{(a)}}\chi$$

Extracting the High-Energy Behaviour of $\sigma_{\rm tot}$

$\mathcal{C}_M$ enters the expression for $\sigma_{\rm tot}$

$$\sigma_{\rm tot} = 2{\rm Re}\int d^2\vec{b}_\perp\, A(s,\vec{b}_\perp) = -4\pi{\rm Re}\int_0^\infty dbb\,\langle\!\langle \mathcal{C}_M(\chi;\vec{b}_\perp;\nu_1,\nu_2)\rangle\!\rangle$$

What is the characteristic b_c?

$$b_c(s) = \max_\alpha R_{\rm eff}^{[\alpha]}(s) = \max_a R_{\rm eff}^{(a)}(s) = \left[\max_a \frac{s^{(a)}-1}{m^{(a)}}\right]\chi = \frac{\tilde{s}-1}{\tilde{m}}\chi$$

If higher-spin ($s^{(a)} > 1$) stable states exist

$$\sigma_{\rm tot} \propto b_c(s)^2 \sim \left(\frac{\tilde{s}-1}{\tilde{m}}\right)^2 \log^2 s$$

If $\tilde{s} < 1$, $\sigma_{\rm tot} \to 0$; if $\tilde{s} = 1$, $\sigma_{\rm tot} \to {\rm const.}$

Extracting the High-Energy Behaviour of $\sigma_{\rm tot}$

$\mathcal{C}_M$ enters the expression for $\sigma_{\rm tot}$

$$\sigma_{\rm tot} = 2{\rm Re} \int d^2\vec{b}_\perp\, A(s,\vec{b}_\perp) = -4\pi{\rm Re} \int_0^\infty dbb\, \langle\langle \mathcal{C}_M(\chi;\vec{b}_\perp;\nu_1,\nu_2)\rangle\rangle$$

What is the characteristic b_c?

$$b_c(s) = \max_\alpha R_{\rm eff}^{[\alpha]}(s) = \max_a R_{\rm eff}^{(a)}(s) = \left[\max_a \frac{s^{(a)}-1}{m^{(a)}}\right]\chi = \frac{\tilde{s}-1}{\tilde{m}}\chi$$

If higher-spin ($s^{(a)} > 1$) stable states exist

$$\sigma_{\rm tot} \propto b_c(s)^2 \sim \left(\frac{\tilde{s}-1}{\tilde{m}}\right)^2 \log^2 s$$

If $\tilde{s} < 1$, $\sigma_{\rm tot} \to 0$; if $\tilde{s} = 1$, $\sigma_{\rm tot} \to {\rm const.}$

Extracting the High-Energy Behaviour of $\sigma_{\rm tot}$

Large-χ, b behaviour encoded in

$$\mathcal{C}_M(\chi;\vec{b}_\perp;\nu_1,\nu_2) \underset{\chi,b\to\infty}{\sim} g(\omega(\chi,z);\nu_1,\nu_2) - 1$$

where $z \equiv e^{(\tilde{s}-1)\chi}e^{-\tilde{m}b}$ and $\omega(\chi,z) \equiv z\left[\log\left(\frac{e^{(\tilde{s}-1)\chi}}{z}\right)\right]^{-\frac{1}{2}} = \frac{e^{(\tilde{s}-1)\chi}e^{-\tilde{m}b}}{\sqrt{\tilde{m}b}}$

One finds that ($\Lambda \equiv e^{-\tilde{m}b_0}$)

$$\sigma_{\rm tot} \simeq \frac{4\pi}{\tilde{m}^2}{\rm Re}\,\langle\!\langle J \rangle\!\rangle \qquad J \underset{\chi\to\infty}{\sim} \int_0^{e^\eta} \frac{dz'}{z'}\log\left(\frac{e^\eta}{\Lambda z'}\right)\left[1 - g(\Lambda z';\nu_1,\nu_2)\right]$$

where $\eta = \frac{1}{2}W(2e^{2(\tilde{s}-1)\chi})$ (*Lambert function* $W(x)$: $x = W(x)e^{W(x)}$).

For large positive x, $W(x) = \log x - \log\log x + \frac{\log\log x}{\log x} + \ldots$, so that

$$\eta = (\tilde{s}-1)\chi - \frac{1}{2}\log[(\tilde{s}-1)\chi] + \frac{\log[(\tilde{s}-1)\chi]}{4(\tilde{s}-1)\chi} + \ldots$$

Look for $\mathcal{O}(\eta^2)$ terms: $J = \frac{1}{2}\eta^2[1 - g_\infty(\nu_1,\nu_2)] + \mathcal{O}(\eta)$

Universal "Froissart-like" Total Cross Section

$$\sigma_{\rm tot} \underset{s\to\infty}{\sim} \frac{2\pi}{\tilde{m}^2}\kappa\,\eta^2 + \mathcal{O}(\eta)\ , \quad \kappa = 1 - {\rm Re}\,\langle\!\langle g_\infty(\nu_1,\nu_2)\rangle\!\rangle$$

Unitarity bound: $|\mathcal{C}_M + 1| = |g| \leq 1 \Rightarrow 0 \leq \kappa \leq 2 \Rightarrow$ bound on $\sigma_{\rm tot}$

$$\sigma_{\rm tot} \underset{s\to\infty}{\lesssim} \frac{4\pi(\tilde{s}-1)^2}{\tilde{m}^2}\log^2\frac{s}{m^2}$$

If ${\rm Re}\,g_\infty(\nu_1,\nu_2) = 0$ (i.e., $\kappa = 1$), $\sigma_{\rm tot}$ is universal and the leading $\mathcal{O}(\eta^2)$ term is entirely determined by the spectrum

$$\sigma_{\rm tot} \underset{s\to\infty}{\sim} \frac{2\pi(\tilde{s}-1)^2}{\tilde{m}^2}\log^2\frac{s}{m^2}$$

True also if g oscillates at infinity, unaffected by small-b behaviour

Universal "Froissart-like" Total Cross Section

$$\sigma_{\rm tot} \underset{s\to\infty}{\sim} \frac{2\pi}{\tilde{m}^2}\kappa\,\eta^2 + \mathcal{O}(\eta)\ , \quad \kappa = 1 - {\rm Re}\,\langle\!\langle g_\infty(\nu_1,\nu_2)\rangle\!\rangle$$

Unitarity bound: $|\mathcal{C}_M + 1| = |g| \le 1 \Rightarrow 0 \le \kappa \le 2 \Rightarrow$ bound on $\sigma_{\rm tot}$

$$\sigma_{\rm tot} \underset{s\to\infty}{\lesssim} \frac{4\pi(\tilde{s}-1)^2}{\tilde{m}^2}\log^2\frac{s}{m^2}$$

If ${\rm Re}\,g_\infty(\nu_1,\nu_2) = 0$ (i.e., $\kappa = 1$), $\sigma_{\rm tot}$ is universal and the leading $\mathcal{O}(\eta^2)$ term is entirely determined by the spectrum

$$\sigma_{\rm tot} \underset{s\to\infty}{\sim} \frac{2\pi(\tilde{s}-1)^2}{\tilde{m}^2}\log^2\frac{s}{m^2}$$

True also if g oscillates at infinity, unaffected by small-b behaviour

Universal "Froissart-like" Total Cross Section

$$\sigma_{\rm tot} \underset{s\to\infty}{\sim} \frac{2\pi}{\tilde{m}^2}\kappa\,\eta^2 + \mathcal{O}(\eta)\ , \quad \kappa = 1 - \mathrm{Re}\,\langle\!\langle g_\infty(\nu_1,\nu_2)\rangle\!\rangle$$

Unitarity bound: $|\mathcal{C}_M + 1| = |g| \leq 1 \Rightarrow 0 \leq \kappa \leq 2 \Rightarrow$ bound on $\sigma_{\rm tot}$

$$\sigma_{\rm tot} \underset{s\to\infty}{\lesssim} \frac{4\pi(\tilde{s}-1)^2}{\tilde{m}^2}\log^2\frac{s}{m^2}$$

If $\mathrm{Re}\,g_\infty(\nu_1,\nu_2) = 0$ (i.e., $\kappa = 1$), $\sigma_{\rm tot}$ is universal and the leading $\mathcal{O}(\eta^2)$ term is entirely determined by the spectrum

$$\sigma_{\rm tot} \underset{s\to\infty}{\sim} \frac{2\pi(\tilde{s}-1)^2}{\tilde{m}^2}\log^2\frac{s}{m^2}$$

True also if g oscillates at infinity, unaffected by small-b behaviour

Subleading Terms

In general, for two colliding hadrons with masses m_a and m_b

$$\sigma^{ab}_{\mathrm{tot}} \underset{s\to\infty}{\sim} \frac{2\pi}{\tilde{m}^2}\kappa\,\eta^2 + \mathcal{O}(\eta)\ , \quad \kappa = 1 - \mathrm{Re}\,\langle\!\langle g_\infty(\nu_1,\nu_2)\rangle\!\rangle$$

where

$$\eta = \frac{1}{2}W(2e^{2(\tilde{s}-1)\chi}) = (\tilde{s}-1)\chi - \frac{1}{2}\log[(\tilde{s}-1)\chi] + \frac{\log[(\tilde{s}-1)\chi]}{4(\tilde{s}-1)\chi} + \ldots$$

and $\chi = \ln(s/s_0^{ab})$ with $s_0^{ab} = m_a m_b$.
Therefore, up to first subleading order,

$$\sigma^{ab}_{\mathrm{tot}} \underset{s\to\infty}{\sim} B\log^2\left(\frac{s}{s_0^{ab}}\right) + C\log\left(\frac{s}{s_0^{ab}}\right)\log\left[\log\left(\frac{s}{s_0^{ab}}\right)\right] + \mathcal{O}\left(\log\left(\frac{s}{s_0^{ab}}\right)\right)$$

with

$$B = \kappa B_{\mathrm{th}}\ , \quad B_{\mathrm{th}} = 2\pi\frac{(\tilde{s}-1)^2}{\tilde{m}^2}\ , \qquad C = \kappa C_{\mathrm{th}}\ , \quad C_{\mathrm{th}} = -2\pi\frac{(\tilde{s}-1)}{\tilde{m}^2}$$

Notice the relations: $B/C = 1-\tilde{s}$ and $2\pi B/C^2 = \tilde{m}^2/\kappa$

Elastic Scattering Amplitude

The elastic scattering amplitude is found to be

$$\mathcal{M}^{ab}(s,t) \underset{s\to\infty,\, t\to 0}{\sim} 4\pi i s\kappa \left(\frac{\eta}{\tilde{m}}\right)^2 \frac{J_1(\varrho)}{\varrho} , \quad \varrho \equiv \frac{\eta\sqrt{-t}}{\tilde{m}} \text{ fixed}$$

One can calculate the total elastic cross section $\sigma_{\rm el}^{ab}$ using

$$\sigma_{\rm el}^{ab}(s) = \int_{-\infty}^{0} dt \frac{d\sigma_{\rm el}^{ab}}{dt}(s,t) , \qquad \frac{d\sigma_{\rm el}^{ab}}{dt}(s,t) = \frac{1}{16\pi s^2}|\mathcal{M}^{ab}(s,t)|^2$$

and assuming that the small-t region gives the dominant contribution:

$$\frac{\sigma_{\rm el}^{ab}}{\sigma_{\rm tot}^{ab}} \underset{s\to\infty}{\sim} \frac{\kappa}{2} \qquad \left[\frac{\sigma_{\rm el}^{pp}}{\sigma_{\rm tot}^{pp}}\Big|_{\rm exp,\, \sqrt{s}=8\,TeV} \simeq 0.27 \right]$$

$(\mathcal{B}^{ab}(\text{slope}) \equiv \frac{d}{dt}\log \frac{d\sigma_{\rm el}^{ab}}{dt}\Big|_{t=0} \Rightarrow \frac{8\pi\mathcal{B}^{ab}}{\sigma_{\rm tot}^{ab}} \sim \frac{1}{\kappa} \qquad [\frac{8\pi\mathcal{B}^{pp}}{\sigma_{\rm tot}^{pp}}|_{\rm exp,\sqrt{s}=7\,TeV} \simeq 1.97])$

If $\kappa < 1$ ($\Rightarrow \sigma_{\rm el}/\sigma_{\rm tot} < 1/2$), the elastic scattering amplitude $\mathcal{M}^{ab}(s,t)$ behaves asymptotically as a *grey disk* with $A_{\rm GD}(s, b < b_c(s) = \frac{\eta}{\tilde{m}}) = \kappa$.

If $\kappa = 1$ we have the so-called *black disk* $\Rightarrow \sigma_{\rm el}/\sigma_{\rm tot} = 1/2$.

If $\kappa > 1$ we have the *antishadowing regime* $\Rightarrow \sigma_{\rm el}/\sigma_{\rm tot} > 1/2$.

Hadronic Spectrum and Total Cross Sections

Maximise $\frac{s^{(a)}-1}{m^{(a)}}$ over asymptotic stable states of QCD *in isolation*

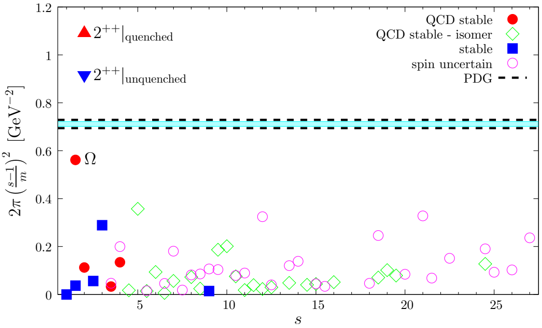

Data from [Nubase (2003), Gregory *et al.* (2012)]

$$\Omega^{\pm} \text{ baryon: } m_\Omega \simeq 1.67 \text{ GeV}, \left(J^P\right)_\Omega = \frac{3}{2}^+$$
$$\Rightarrow B_{\rm th}^{\Omega} = \frac{\pi}{2m_\Omega^2} \simeq 0.56 \text{ GeV}^{-2} \text{ [0.22 mb]}$$

vs. $B_{\rm exp} \simeq 0.69 \div 0.73 \text{ GeV}^{-2}$ [$0.27 \div 0.29$ mb]

"Froissart-like" Bound

Froissart-Łukaszuk-Martin bound

$$\lim_{s\to\infty} \frac{\sigma_{\rm tot}}{\log^2 \frac{s}{m^2}} \le \frac{\pi}{m_\pi^2} \simeq 59\ \mathrm{mb}$$

Our "Froissart-like" bound is much more restrictive $(B_{\rm exp} = 0.27 \div 0.29\,\mathrm{mb}\ )$

$$\lim_{s\to\infty} \frac{\sigma_{\rm tot}}{\log^2 \frac{s}{m^2}} \le 2B_{\rm th}^{\Omega} = \frac{\pi}{m_\Omega^2} \simeq 0.44\ \mathrm{mb}$$

In the $N_f = 2$ chiral limit our "Froissart-like" bound is stable

- masses of nuclei/baryons/non-Goldstone mesons expected to change only by a few MeV
- the presence of massless pions can make some particle unstable, not the other way around
- massless spin-0 particles are harmless, and do not have to be included in the maximisation
- Ω expected to remain stable and with approximately the same mass, so it is expected to still be the dominant particle

Quenched and Large-N_c Limits

Quenched limit

The description of hadrons in terms of dipoles is (probably) most naturally justified in the *quenched* limit of the theory:

- Quark masses $\to \infty$, B from the *glueball* spectrum of YM theory
- Glueball 3^{+-} ($m_{g(3^{+-})} \simeq 3.55$ GeV) $\Rightarrow B_{\rm th}^{g(3^{+-})} = 0.78$ mb
- Or, maybe (if, for some reason, states for which one-particle contributions are nonzero should be considered to be "dominant"): Glueball 2^{++} ($m_{g(2^{++})} \simeq 2.40$ GeV) $\Rightarrow B_{\rm th}^{g(2^{++})} = 0.42$ mb

Large-N_c limit

- Large-s limit first, large-N_c next: $s \to \infty$ / $N_c \to \infty$
- $B_{\rm th}$ well defined for all (finite) N_c as the stable spectrum is finite
- Ω baryon likely to remain stable in the large-N_c limit: $J_\Omega = \frac{N_c}{2}$, $m_\Omega \sim N_c \Rightarrow B_{\rm th}^{\Omega} = \mathcal{O}(N_c^0)$
- Also, in the *quenched* theory: $m_g = \mathcal{O}(N_c^0) \Rightarrow B_{\rm th}^{g} = \mathcal{O}(N_c^0)$ (Quenched and large-N_c are *not* equivalent for $\sigma_{\rm tot}$!)
- In contrast with expected $\mathcal{O}(\frac{1}{N_c^2})$ in the limit $N_c \to \infty$ / $s \to \infty$

Best-Fit Analysys: Parametrization

We have done best fits to hadronic scattering data using the following parametrization for the total cross section:

$$\sigma_{\rm tot}(s) = \sigma_{\rm Regge}(s) + \sigma_{\rm HE}(s) \ ,$$

$$\sigma_{\rm Regge}^{a^{\pm}b}(s) = A_1^{ab} \left(\frac{s}{s_0^{ab}} \right)^{-b_1} \mp A_2^{ab} \left(\frac{s}{s_0^{ab}} \right)^{-b_2} + A_{\mathbb{P}}^{ab} \ ,$$

$$\sigma_{\rm HE}^{a^{\pm}b}(s) = \kappa \left\{ B \log^2 \left(\frac{s}{s_0^{ab}} \right) + C \log \left(\frac{s}{s_0^{ab}} \right) \log \left[\log \left(\frac{s}{s_0^{ab}} \right) \right] \right\} + Q^{ab} \log \left(\frac{s}{s_0^{ab}} \right) \ ,$$

where: $a^+ \equiv a$, $a^- \equiv \bar{a}$ and $s_0^{ab} = m_a m_b$.
A_i^{ab} (mb), b_i (dimensionless) and $A_{\mathbb{P}}^{ab}$ (mb) are always free parameters to be determined in the fits.
The parameters B (mb), C (mb), Q^{ab} (mb) and κ (dimensionless) can be fixed or free, depending on the particular type of best fit.

Best-Fit Analysis: Dataset

Information about the reactions in our dataset (minimum energy, maximum energy and number of points for each reaction):

Reaction	$\sqrt{s_{\text{min}}}$ (GeV)	$\sqrt{s_{\text{max}}}$ (GeV)	# points
pp	5.01	8000	112
$\bar{p}p$	5.16	1800	59
pn	5.30	26.40	34
$\bar{p}n$	5.18	22.98	33
π^+p	5.21	25.28	50
π^-p	5.03	34.67	95
K^+p	5.13	24.14	40
K^-p	5.11	24.14	63
K^+n	5.24	24.16	28
K^-n	5.11	24.16	36
		Total:	559

Best-Fit Analysis: Results for pp and $\bar{p}p$ Scattering

Results of fits with LT, SLT and QLT to σ_{tot} data of pp and $\bar{p}p$ scattering:

	Fits to σ_{tot}		
	LT	SLT	QLT
B	0.2269(38)	0.349(29)	0.311(19)
C	0 (fixed)	-0.95(21)	0 (fixed)
κ	1 (fixed)	1 (fixed)	1 (fixed)
Q	0 (fixed)	0 (fixed)	-2.40(48)
b_1	0.342(15)	0.560(76)	0.586(89)
b_2	0.539(15)	0.541(16)	0.541(16)
A_1	56.8(1.7)	64.4(8.2)	60.6(8.7)
A_2	35.2(2.5)	35.6(2.5)	35.6(2.5)
$A_{\mathbb{P}}$	24.77(60)	35.7(2.0)	41.7(3.0)
χ^2/ν	0.972	0.933	0.934
ν	165	164	164

Best-Fit Analysis: Results for pp and $\bar{p}p$ Scattering

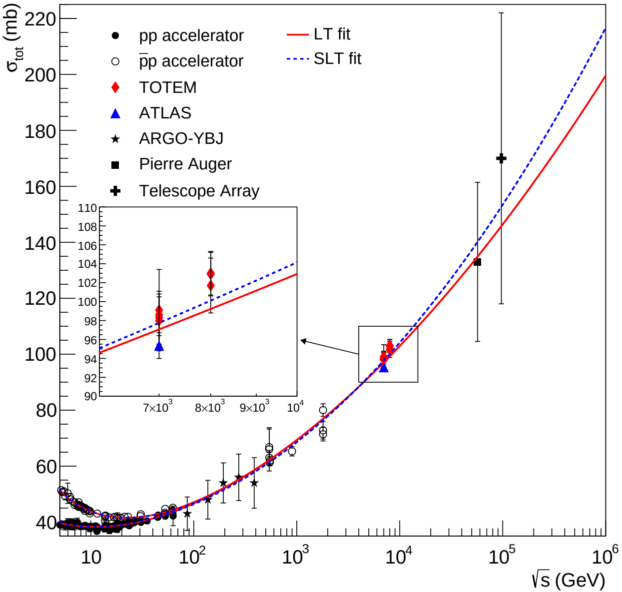

Best-Fit Analysis: Results for pp and $\bar{p}p$ Scattering

Results of fits with $\mathrm{LT_{th}}$, $\mathrm{SLT_{th}}$ and $\mathrm{SLT}_{\mathrm{th},\kappa}$ (B and C fixed to their theoretical values B_{th} and C_{th}, $Q = 0$) to σ_{tot} data of pp and $\bar{p}p$ scattering:

	$\Omega^{\pm}$ baryon			2^{++} glueball	3^{+-} glueball
	$\mathrm{LT_{th}}$	$\mathrm{SLT_{th}}$	$\mathrm{SLT}_{\mathrm{th},\kappa}$	$\mathrm{SLT}_{\mathrm{th},\kappa}$	$\mathrm{SLT}_{\mathrm{th},\kappa}$
B_{th}	0.22 (fixed)	0.22 (fixed)	0.22 (fixed)	0.42 (fixed)	0.78 (fixed)
C_{th}	0 (fixed)	-0.44 (fixed)	-0.44 (fixed)	-0.42 (fixed)	-0.39 (fixed)
κ	1 (fixed)	1 (fixed)	1.377(18)	0.6159(96)	0.3097(51)
κB_{th}	0.22 (fixed)	0.22 (fixed)	0.303(4)	0.259(4)	0.242(4)
Q	0 (fixed)	0 (fixed)	0 (fixed)	0 (fixed)	0 (fixed)
b_1	0.365(10)	0.743(20)	0.548(20)	0.385(17)	0.361(17)
b_2	0.539(15)	0.528(16)	0.540(15)	0.539(15)	0.539(15)
A_1	58.5(1.7)	115.3(8.5)	57.5(3.2)	56.0(2.2)	56.3(2.0)
A_2	35.3(2.5)	33.7(2.4)	35.4(2.5)	35.3(2.4)	35.2(2.4)
$A_{\mathbb{P}}$	25.75(21)	35.862(74)	32.17(29)	28.13(46)	26.38(55)
χ^2/ν	0.987	3.59	0.937	0.957	0.965
ν	166	166	165	165	165

Best-Fit Analysis: Results for pp and $\bar{p}p$ Scattering

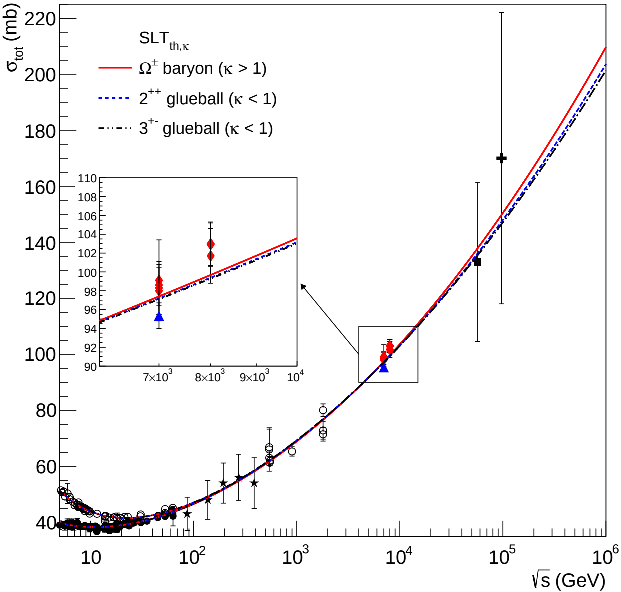

Best-Fit Analysis: Results for All Reactions

Results of fits with $\mathrm{LT_{th}}$, $\mathrm{SLT_{th}}$ and $\mathrm{SLT_{th,\kappa}}$ (B and C fixed to their theoretical values B_{th} and C_{th}, $Q = 0$) to σ_{tot} data for all hadron-hadron reactions:

	$\Omega^{\pm}$ baryon			2^{++} glueball	3^{+-} glueball
	$\mathrm{LT_{th}}$	$\mathrm{SLT_{th}}$	$\mathrm{SLT_{th,\kappa}}$	$\mathrm{SLT_{th,\kappa}}$	$\mathrm{SLT_{th,\kappa}}$
B_{th}	0.22 (fixed)	0.22 (fixed)	0.22 (fixed)	0.42 (fixed)	0.78 (fixed)
C_{th}	0 (fixed)	-0.44 (fixed)	-0.44 (fixed)	-0.42 (fixed)	-0.39 (fixed)
κ	1 (fixed)	1 (fixed)	1.439(23)	0.653(12)	0.3303(64)
κB_{th}	0.22 (fixed)	0.22 (fixed)	0.317(5)	0.274(5)	0.258(5)
Q	0 (fixed)	0 (fixed)	0 (fixed)	0 (fixed)	0 (fixed)
b_1	0.2744(66)	0.554(13)	0.292(14)	0.249(13)	0.234(12)
b_2	0.5141(97)	0.515(11)	0.514(10)	0.513(11)	0.513(11)
χ^2/ν	1.108	1.966	1.071	1.062	1.061
ν	533	533	532	532	532

Best-Fit Analysis: Results for All Reactions

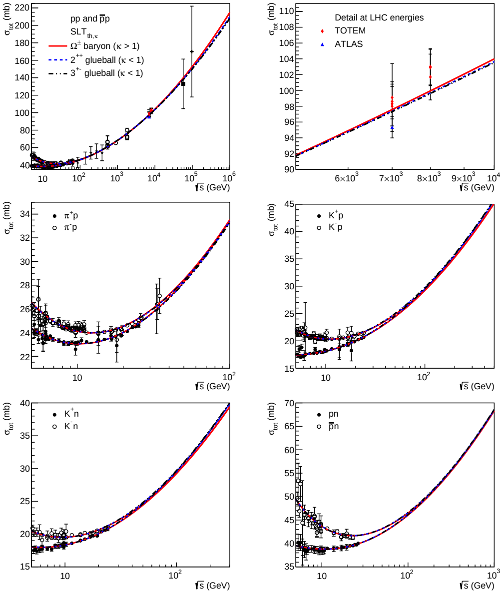

Best-Fit Analysis: Results for the Ratio $\sigma_{\rm el}/\sigma_{\rm tot} = \kappa/2$

Ratio $\sigma_{\rm el}/\sigma_{\rm tot} = \kappa/2$, with κ determined from the fit LT (considering $B = \kappa B_{\rm th}$, i.e., $\kappa = B/B_{\rm th}$) and from the fits $\mathrm{SLT}_{\mathrm{th},\kappa}$ and $\mathrm{QSLT}_{\mathrm{th},\kappa}$ to pp and $\bar{p}p$ data only, and also from fits to data for all reactions:

	Fits to $pp/\bar{p}p$ data only		Fits to all reactions	
	LT		LT	
$\Omega^{\pm}$ baryon	0.5157(86)		0.553(10)	
2^{++} glueball	0.2701(45)		0.2896(55)	
3^{+-} glueball	0.1454(24)		0.1560(29)	
	$\mathrm{SLT}_{\mathrm{th},\kappa}$	$\mathrm{QSLT}_{\mathrm{th},\kappa}$	$\mathrm{SLT}_{\mathrm{th},\kappa}$	$\mathrm{QSLT}_{\mathrm{th},\kappa}$
$\Omega^{\pm}$ baryon	0.6885(91)	0.765(50)	0.720(12)	0.770(55)
2^{++} glueball	0.3080(48)	0.385(25)	0.3265(60)	0.387(26)
3^{+-} glueball	0.1548(26)	0.203(13)	0.1652(32)	0.204(12)

Conclusions and Outlook

Main results:

- If higher-spin ($\tilde{s} > 1$) *stable* states exist, then:
  $\sigma_{\rm tot} \sim B \log^2 s + C \log s \log(\log s) + \mathcal{O}(\log s)$, with

$$B = \kappa B_{\rm th}\ , \quad B_{\rm th} = 2\pi \frac{(\tilde{s}-1)^2}{\tilde{m}^2}\ , \quad C = \kappa C_{\rm th}\ , \quad C_{\rm th} = -2\pi \frac{(\tilde{s}-1)}{\tilde{m}^2}$$

  where $\frac{\tilde{s}-1}{\tilde{m}} = \max \frac{s^{(a)}-1}{m^{(a)}}$ and $\frac{\sigma_{\rm el}}{\sigma_{\rm tot}} \sim \frac{\kappa}{2}$ $\quad (0 \le \kappa \le 2)$

- Reasonable possibilities for the relevant state (of mass $\tilde{m}$ and spin $\tilde{s}$):
  $\Omega^{\pm}$ baryon , 2^{++} glueball , 3^{+-} glueball

- Good best fits to data (both for $pp/\bar{p}p$ reactions only and also including all hadron-hadron reactions) have been obtained using the above-written asymptotic expression for $\sigma_{\rm tot}$, with κ treated as a free parameter:
  - $\Omega^{\pm}$ baryon: $B \sim 0.3$ mb, $\frac{\kappa}{2} \sim 0.7 \Longrightarrow$ *anti-shadowing* scenario?
  - 2^{++} glueball: $B \sim 0.27$ mb, $\frac{\kappa}{2} \sim 0.3 \Longrightarrow$ *grey-disk* scenario?
  - 3^{+-} glueball: $B \sim 0.26$ mb, $\frac{\kappa}{2} \sim 0.16 \Longrightarrow$ *grey-disk* scenario?

(We recall that: $B_{\rm PDG} \simeq 0.27$ mb, $\sigma_{\rm el}^{pp}/\sigma_{\rm tot}^{pp}|_{{\rm exp},\sqrt{s}=8\,{\rm TeV}} \simeq 0.27$)

Conclusions and Outlook

Open issues:

- Validity of our technical assumptions?
- Which is the *true* relevant state?
  The $\Omega^{\pm}$ baryon? Some glueball (2^{++}, 3^{+-},...)?
  Or, maybe, something else?
- More detailed fits (and, therefore, more high-energy data) will be necessary to settle this question...

References

- K. A. Olive *et al.* [Particle Data Group Collaboration]
  Chin. Phys. C **38** (2014) 090001
- G. Antchev et al. (TOTEM collaboration)
  Europhys. Lett. **101** (2013) 21002
  Phys. Rev. Lett. **111** (2013) 012001
- K. Igi and M. Ishida
  Phys. Rev. D **66** (2002) 034023
- M. Froissart
  Phys. Rev. **123** (1961) 1053
- O. Nachtmann
  Ann. Phys. **209** (1991) 436
- H. G. Dosch, E. Ferreira and A. Krämer
  Phys. Rev. D **50** (1994) 1992
- H. Verlinde and E. Verlinde
  hep–th/9302104
- M. Rueter and H. G. Dosch
  Phys. Lett. B **380** (1996) 177
- E. Meggiolaro
  Z. Phys. C **76** (1997) 523
- E. Meggiolaro
  Nucl. Phys. B **707** (2005) 199
- M. Giordano and E. Meggiolaro
  Phys. Lett. B **675** (2009) 123
- M. Giordano and E. Meggiolaro
  Phys. Rev. D **74** (2006) 016003
- E.R. Berger and O. Nachtmann
  Eur. Phys. J. C **7** (1999) 459
- A. I. Shoshi, F. D. Steffen, H. G. Dosch and H. J. Pirner
  Phys. Rev. D **68** (2003) 074004
- E. Shuryak and I. Zahed
  Phys. Rev. D **62** (2000) 085014
- M. Giordano and E. Meggiolaro
  Phys. Rev. D **81** (2010) 074022
- M. Giordano and E. Meggiolaro
  Phys. Rev. D **78** (2008) 074510
- R. A. Janik and R. Peschanski
  Nucl. Phys. B **565** (2000) 193; **586** (2000) 163
- M. Giordano and R. Peschanski
  JHEP **05** (2010) 037
- M. Giordano, E. Meggiolaro and N. Moretti
  JHEP **09** (2012) 031
- G. Audi, O. Bersillon, J. Blachot and A. H. Wapstra
  Nucl. Phys. A **729** (2003) 3
- E. Gregory *et al.*
  JHEP **10** (2012) 170